Nanomaterials **2014**, *4*, 46-54; doi:10.3390/nano4010046

OPEN ACCESS

nanomaterials

ISSN 2079-4991

www.mdpi.com/journal/nanomaterials

Article

Effect of Low-Frequency AC Magnetic Susceptibility and Magnetic Properties of CoFeB/MgO/CoFeB Magnetic Tunnel Junctions

Yuan-Tsung Chen *, Sung-Hao Lin and Tzer-Shin Sheu

Department of Materials Science and Engineering, I-Shou University, Kaohsiung 840, Taiwan; E-Mails: isu10107009m@cloud.isu.edu.tw (S.H.L.); sheu415@isu.edu.tw (T.S.S.)

* Author to whom correspondence should be addressed; E-Mail: ytchen@isu.edu.tw; Tel: +886-765-777-11 (ext. 3119); Fax: +886-765-784-44.

Received: 14 November 2013; in revised form: 19 December 2013 / Accepted: 24 December 2013 / Published: 2 January 2014

Abstract: In this investigation, the low-frequency alternate-current (AC) magnetic susceptibility (χ_{ac}) and hysteresis loop of various MgO thickness in CoFeB/MgO/CoFeB magnetic tunneling junction (MTJ) determined coercivity (H_c) and magnetization (M_s) and correlated that with χ_{ac} maxima. The multilayer films were sputtered onto glass substrates and the thickness of intermediate barrier MgO layer was varied from 6 to 15 Å. An experiment was also performed to examine the variation of the highest χ_{ac} and maximum phase angle (θ_{max}) at the optimal resonance frequency (f_{res}), at which the spin sensitivity is maximal. The results reveal that χ_{ac} falls as the frequency increases due to the relationship between magnetization and thickness of the barrier layer. The maximum χ_{ac} is at 10 Hz that is related to the maximal spin sensitivity and that this corresponds to a MgO layer of 11 Å. This result also suggests that the spin sensitivity is related to both highest χ_{ac} and maximum phase angle. The corresponding maximum of χ_{ac} is related to high exchange coupling. High coercivity and saturation magnetization contribute to high exchange-coupling χ_{ac} strength.

Keywords: magnetic tunnel junctions (MTJs); exchange coupling; low-frequency alternate-current (AC) magnetic susceptibility (χ_{ac}); resonance frequency (f_{res})

---

1. Introduction

Since 1995, the tunneling magnetoresistance (TMR) effect has been extensively discussed, and it has been exploited in much of our modern technology [1,2]. In the past, increasing attention has been paid to ferromagnetic exchange coupling in magnetic fields [3,4], and the discovery of spintronics has led to a rapid increase in the number of exchange coupling issues. A magnetic tunneling junction (MTJ) has a trilayer structure that comprises a top free ferromagnetic (FM1) layer, an insulating tunneling barrier layer (spacer), and a bottom pinned ferromagnetic (FM2) layer. It has a great potential for use in magnetoresistance random access memory (MRAM). It provides many advantages, such as low loss energy, lack of volatility and semi-permanence features, and can be used in high-density magnetic read heads [5–7]. The first demonstrated MgO based tunnel junctions are Parkin *et al.* [8] and Yuasa *et al.* [9]. The mechanism of TMR in MgO based junctions is explained by Butler *et al.* [10]. In the past, TMR based on CoFeB/MgO/CoFeB MTJ has attracted considerable attention. For example, a previous study found that the magnetron sputtering of CoFeB/MgO/CoFeB at room temperature (RT) yielded a high TMR ratio [11,12]. Lee *et al.* [13] also achieved a TMR ratio of 500% at RT. Furthermore, the fabrication of high-quality junctions requires a superior ferromagnetic layer with a high spin polarization, a crystalline ordering, and a sufficient indirect spin exchange-coupling between the FM1 and FM2 layers [14–17]. The defects in the tunnel barrier material can lead to electron trapping and resistance fluctuations and induce field-dependent 1/f noise [18]. The origin of 1/f power spectrum is attributed to charge traps occurring in the barrier layer or near the interfaces between barrier and magnetic layers at low frequencies [18–23]. The alternate-current (AC) susceptibility is related to magnetic noise and exchange-coupling interaction. The high AC susceptibility can enhance a strong dipole-dipole interaction effect [24]. Moreover, a proper exchange-coupling interaction can induce a large signal-to-noise ratio [25]. However, the external stress acting on magnetic element can induce magnetic susceptibility variation of ferromagnetic layers and disturb spectral power noise of read head device. At low frequencies, the spectral power noise is dependent on free and fixed ferromagnetic layers of hysteresis loop owing to thermal magnetization fluctuations. The origin of magnetic fluctuations is excited hopping of magnetic domain walls. However, most of MTJ research has focused on the TMR, whereas the relative low-frequency alternate-current (AC) magnetic susceptibility (χ_{ac}) has rarely been examined. The low field AC measurement at low frequencies is related to the spin sensitivity of MTJ devices [18]. The low-frequency AC magnetic susceptibility (χ_{ac}) and hysteresis loop of CoFeB/MgO/CoFeB are worthwhile to study. This investigation focuses on the maximum χ_{ac}, the optimal resonance frequency (f_{res}) and maximum phase angle (θ_{max}) for various MgO barrier thicknesses (6, 8, 11, 13, and 15 Å). The maximum χ_{ac} is 0.7 at the optimal resonant frequency of 10 Hz and the maximum phase angle is 228° at an MgO thickness of 11 Å. These values are larger than compared for $Fe_{40}Pd_{40}B_{20}$(*X* Å)/ZnO(500 Å) and suitable for low-frequency magnetic media applications [26]. The magnetic material under the external AC magnetic field shows a magnetic property called multiple-frequency AC magnetic susceptibility χ_{ac} [27]. The origin of χ_{ac} is due to the association between magnetic spin interactions [27]. The frequency of the applied AC magnetic field equals the frequency of oscillation of the magnetic dipole. The maximum χ_{ac} value is corresponding to optimal resonance frequency, increasing spin sensitivity at optimal f_{res}. It means that the optimal f_{res} is associated with maximal spin sensitivity.

2. Results and Discussion

Figure 1 presents the χ_{ac} amplitude of the CoFeB/MgO/CoFeB MTJ for different thicknesses of the MgO layer at frequencies in the range 10 to 25,000 Hz. The lowest measured frequency is 10 Hz and the smallest step frequency is 20 Hz at low frequencies for used χ_{ac} measurement. The maxima χ_{ac} at the optimal resonance frequency has the following physical meaning. At low frequencies, the resultant alternate-current (AC) magnetic dipole moment is contributed from the oscillation of volume magnetic dipole moment inside each domain. The applied AC magnetic field acts a driving force. The magnetic interactions among domains act restored. There exists a resonant frequency as a driving force acting to the system. Thus, the frequency of the peak of the low-frequency magnetic susceptibility corresponds to the resonant frequency of the oscillation of the magnetic dipole moment inside domains. The χ_{ac} peak indicates the spin exchange-coupling interaction and dipole moment of domain under frequency [27]. It is reasonably concluded that the physical meaning peaks of the low frequency susceptibility indicate the magnetic exchange coupling between two CoFeB layers. The results suggest that an excitation frequency of 10 to 30 Hz maximizes the χ_{ac} of the magnetic exchange-coupled signal, and as the frequency increases above 30 Hz, the χ_{ac} obtained from the signal declines, suggesting that the CoFeB/MgO/CoFeB MTJ is suited to use at low frequencies. The optimal maximum susceptibility, at frequencies in the range of 10 to 30 Hz, can be utilized in inductors and transformers [28,29].

Figure 1. Measured low-frequency alternate-current magnetic susceptibility (χ_{ac}) of CoFeB/MgO/CoFeB as a function of thickness of MgO barrier layer.

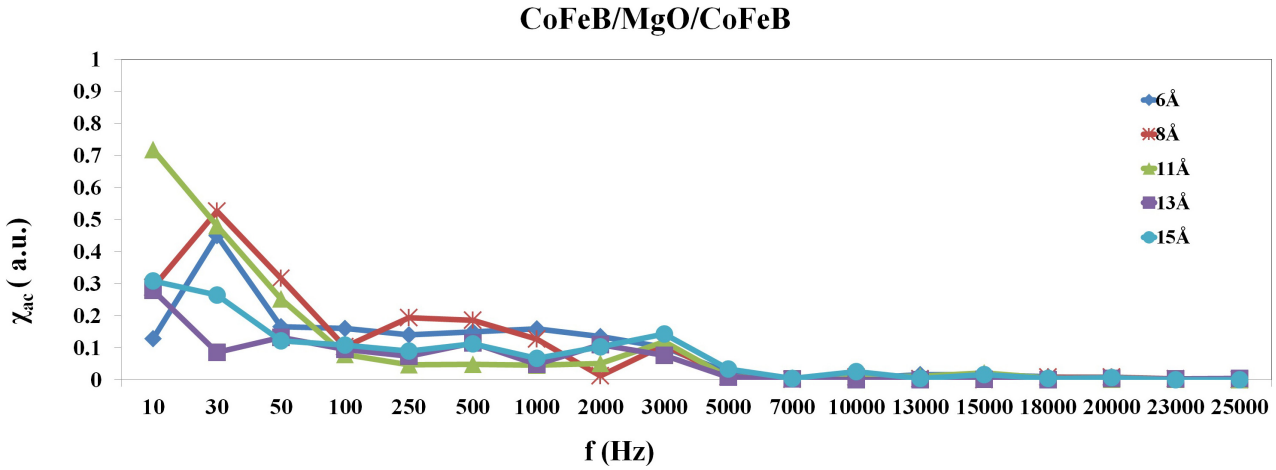

Briefly, the maximum χ_{ac} at the optimal resonant frequency (f_{res}), f_{res} corresponds to the maximum spin sensitivity. Therefore, Figure 2 plots the highest χ_{ac} as a function of MgO thickness. The resonance peak of origin 10 Hz represents to initial spin exchange coupling status. The maximum χ_{ac} value at 6 Å is 0.44, at 8 Å is 0.52, at 11 Å is 0.71, at 13 Å is 0.27, and at 15 Å is 0.3. These findings are known to follow from indirect interactions of magnetic moment. The indirect interactions of magnetic moment mean the spin exchange interaction between free CoFeB and pinned CoFeB layers, which indicate a strong moment interactions can induce a high magnetic susceptibility [24]. The susceptibility peaks relate to the exchange interaction between the two layers closely. The high χ_{ac} peaks are corresponding to high exchange coupling.

Figure 2. Maximum χ_{ac} as a function of thickness of MgO barrier layer.

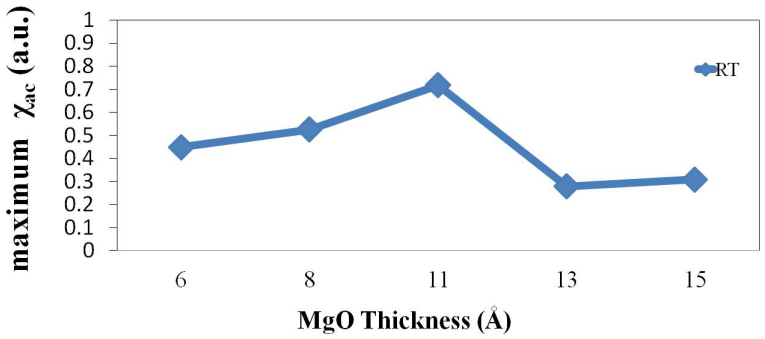

The phase angle (θ) has the following physical meaning. When a magnetic material is in an external magnetic field, the magnetic dipole moment tends to lie in the direction of the interaction of the magnetic moment with the external field. When an external AC magnetic field is applied, and the AC frequency is not too high compared to microwave frequencies, the magnetic dipole moment oscillates. The frequency of the applied AC magnetic field equals the frequency of oscillation of magnetic dipole. However, the direction of instantaneous magnetic dipole is not the same as the direction of the applied magnetic field. The phase angle denotes the difference [29]. Figure 3 plots the corresponding maximum phase angle (θ_{max}) between magnetic field and magnetization as a function of MgO thickness for maximal χ_{ac}. The high χ_{ac} ensures high spin sensitivity to an increase in the phase angle. Restated, by increasing the phase angle improved the sensitivity to detect the behavior of an electron spin. In summary, the results concerning the phase angle are consistent with trend of χ_{ac}.

Figure 3. Variation of maximum χ_{ac} with maximum phase angle (θ).

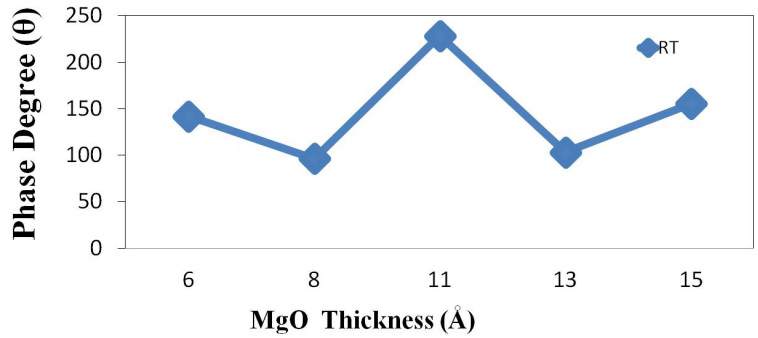

Table 1 presents the important parameters of CoFeB/MgO/CoFeB MTJ. From this Table, an MgO thickness of 11 Å is the best of various MgO thicknesses from 6 to 15 Å. The maximum χ_{ac} of indirect exchange-coupling susceptibility of FM1 and FM2 is 0.7, corresponding to a resonant frequency of 10 Hz and a maximum phase angle of 228.5°. According to previous study, it indicates that susceptibility is associated with 1/f noise due to electron trap in the tunnel barrier [18]. It is related to electron traps and defects in the tunnel barrier but not related to the magnetization fluctuations, which suggests that the quality of the tunneling barrier is an important parameter in reducing low-frequency noise in magnetic tunnel junctions. According to the result, this CoFeB/MgO/CoFeB MTJ is suitable for components and low-frequency magnetic device applications [30].

Table 1. Maximum χ_{ac} value, maximum phase angle, and corresponding optimal resonance frequency for various MgO barrier thicknesses.

MgO (Å)	Maximum χ_{ac} (a.u.)	Maximun phase angle θ_{max} (degree)	Highest χ_{ac} corresponding optimal resonance frequency f_{res} (Hz)
6 Å	0.44	142.24	30 Hz
8 Å	0.52	96.44	30 Hz
11 Å	0.71	228.59	10 Hz
13 Å	0.27	103.47	10 Hz
15 Å	0.30	155.44	10 Hz

Figure 4a shows the hysteresis loop of CoFeB(75 Å)/MgO(11 Å)/CoFeB(75 Å) MTJ. From this figure, the two-step characteristic of hysteresis loop is indicated that the spin rotated situation between two CoFeB layers at saturated magnetic magnetization by external field (H). Moreover, the H1, H2, H3, and H4 of Figure 4a indicate the coercive fields of the two CoFeB layers, respectively. The H_c value of free CoFeB layer denotes (H2 + H4)/2. The H_c value of pinned CoFeB layer is (H1 + H3)/2. The H_c value between two CoFeB layers initially increased at MgO thicknesses from 6 to 11 Å and decreased at MgO thicknesses from 11 to 15 Å. It can be reasonably concluded that high H_c value means high exchange-coupling χ_{ac} strength. High H_c strength requires a large external field to changing the spin arrangement. From Figure 4b, it suggests that the H_c of MTJ is varied by various MgO thicknesses. The result of Figure 4b is consistent with Figure 2. According to the results of Figures 2 and 4b, they indicate that maximum χ_{ac} means a high magnetic exchange coupling between two CoFeB layers and induces a corresponding high H_c. The saturation magnetization (M_s) between two CoFeB layers is also shown the same trend to concave-down feature, which is shown in Figure 4c. From the result of Figure 4, it indicates that high M_s presents to high exchange-coupling χ_{ac} strength and high H_c value.

Figure 4. The essential magnetic properties of magnetic tunneling junction are (**a**) hysteresis loop of MTJ, (**b**) coercivity value, and (**c**) saturation magnetization.

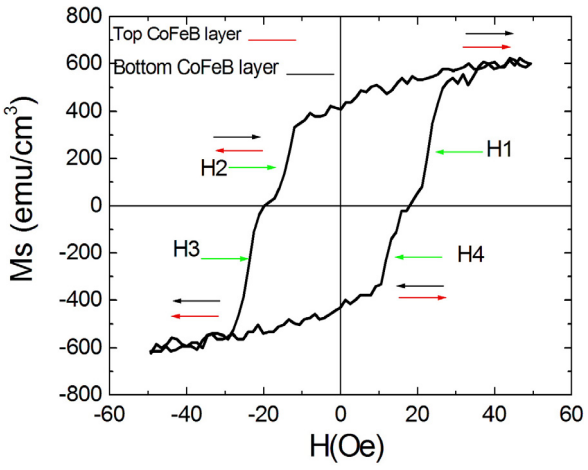

(**a**)

Figure 4. *Cont.*

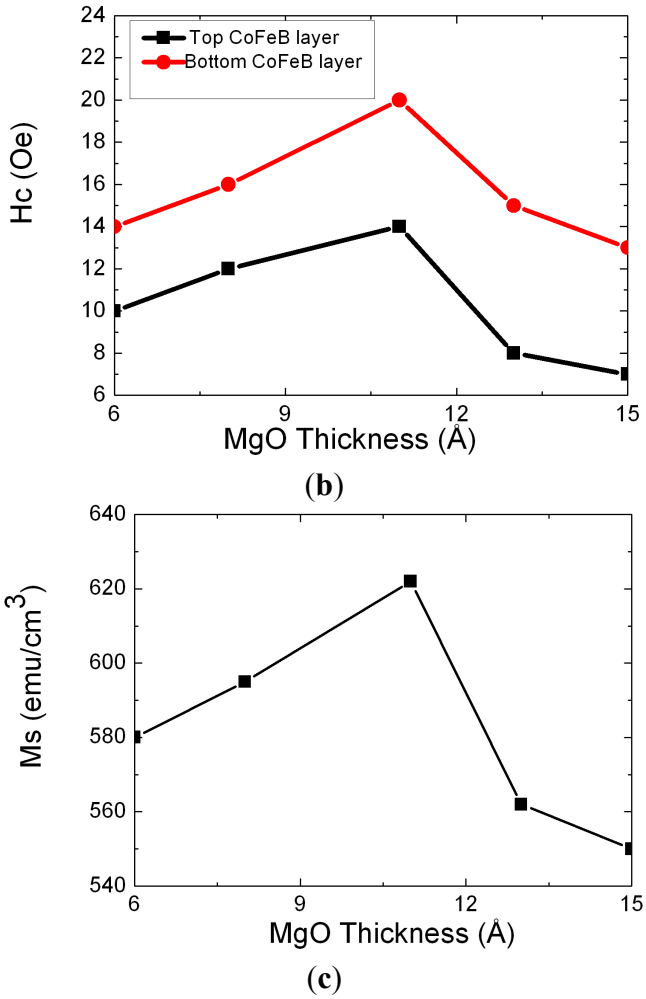

3. Experimental Section

A multilayer MTJ was sputtered on a glass substrate by a DC and RF magnetron sputtering system. The chamber pressure was typically under 1×10^{-7} Torr and the Ar-working chamber pressure was 5×10^{-3} Torr. The MTJ structure was glass/CoFeB(75 Å)/MgO(*d*)/CoFeB(75 Å) with *d* = 6, 8, 11, 13 and 15 Å. The atomic composition of the CoFeB alloy target was 40 atom % Co, 40 atom % Fe, and 20 atom % B. In the fabrication of MgO barrier, the initial metal magnesium (Mg) target was deposited on the bottom of ferromagnetic electrode, and then deposited a magnesium oxide (MgO) layer was formed by RF sputtering reaction in an oxidizing atmosphere using an Ar/O_2 with a mixing ratio of 9:16. The in-plane low-frequency alternate-current magnetic susceptibility (χ_{ac}) of MTJ was studied using an χ_{ac} analyzer (X_{ac}Quan, MagQu, Taiwan). First, the referenced standard sample is calibrated by an χ_{ac} analyzer with an external field. Then, the measured sample is inserted to χ_{ac} analyzer. The driving frequency ranged from 10 to 25,000 Hz. The minimum frequency step is 20 Hz and that the frequency minimum is 10 Hz. The χ_{ac} is determined through the magnetization measurement. All measured samples had the same shape and size to eliminate the demagnetization factor. The χ_{ac} valve is arbitrary unit (a.u.), because the χ_{ac} result is corresponding to referenced standard sample. It is a comparative valve. Moreover, the in-plane coercivity (H_c) and saturation magnetization (M_s) of the two CoFeB layers

were obtained using a superconducting quantum interference device (SQUID, Quantum Design MPMS5, San Diego, CA, USA).

4. Conclusions

The MgO barrier layer thickness in CoFeB/MgO/CoFeB MTJs was varied to measure low-frequency alternate-current magnetic susceptibility and magnetic properties. The highest χ_{ac} was obtained at a thickness of 11 Å, corresponding to an optimal resonance frequency of 10 Hz and a maximum phase angle of 228.5°. The best resonance frequencies are from 10 to 30 Hz, and this range of frequencies is useful for transformers, sensors, and magnetic read heads. Additionally, the important low-frequency alternate-current susceptibility and magnetic results demonstrate that the indirect spin exchange coupling of top CoFeB and bottom CoFeB layers in CoFeB/MgO/CoFeB oscillates.

Acknowledgements

This work was supported by the National Science Council, under Grant No. NSC100-2112-M-214-001-MY3 and No. NSC 102-2815-C-214-009-M.

Conflicts of Interest

The authors declare no conflict of interest.

References

1. Miyazaki, T.; Tezuka, N. Giant magnetic tunneling effect in Fe/Al_2O_3/Fe junction. *J. Magn. Magn. Mater.* **1995**, *139*, L231–L234.
2. Moodera, J.S.; Kinder, L.R.; Wong, T.M.; Meservey, R. Large magnetoresistance at room temperature in ferromagnetic thin film tunnel junctions. *Phys. Rev. Lett.* **1995**, *74*, 3273–3276.
3. Katayama, T.; Yuasa, S.; Velev, J.; Zhuravlev, M.Y.; Jaswal, S.S.; Tsymbal, E.Y. Interlayer exchange coupling in Fe/MgO/Fe magnetic tunnel junctions. *Appl. Phys. Lett.* **2006**, *89*, 112503:1–112503:3.
4. Zhuravlev, M.Y.; Tsymbal, E.Y.; Vedyayev, A.V. Impurity-assisted interlayer exchange coupling across a tunnel barrier. *Phys. Rev. Lett.* **2005**, *94*, 026806:1–026806:4.
5. Matsumoto, R.; Hamada, Y.; Mizuguchi, M.; Shiraishi, M.; Maehara, H.; Tsunekawa, K.; Djayaprawira, D.D.; Watanabe, N.; Kurosaki, Y.; Nagahama, T.; *et al*. Tunneling spectra of sputter-deposited CoFeB/MgO/CoFeB magnetic tunnel junctions showing giant tunneling magnetoresistance effect. *Solid State Commun.* **2005**, *136*, 611–615.
6. Aoki, T.; Ando, Y.; Watanabe, D.; Oogane, M.; Miyazaki, T. Spin transfer switching in the nanosecond regime for CoFeB/MgO/CoFeB ferromagnetic tunnel junctions. *J. Appl. Phys.* **2008**, *103*, 103911:1–103911:4.
7. You, C.Y.; Goripati, H.S.; Furubayashi, T.; Takahashi, Y.K.; Hono, K. Exchange bias of spin valve structure with a top-pinned $Co_{40}Fe_{40}B_{20}$/IrMn. *Appl. Phys. Lett.* **2008**, *93*, 012501:1–012501:3.

8. Parkin, S.S.P.; Kaiser, C.; Panchula, A.; Rice, P.M.; Hughes, B.; Samant, M.; Yang, S.H. Giant tunneling magnetoresistance at room temperature with MgO (100) tunnel barriers. *Nat. Mater.* **2004**, *3*, 862–867.
9. Yuasa, S.; Nagahama, T.; Fukushima, A.; Suzuki, Y.; Ando, K. Giant room-temperature magnetoresistance in single-crystal Fe/MgO/Fe magnetic tunnel junctions. *Nat. Mater.* **2004**, *3*, 868–871.
10. Butler, W.H.; Zhang, X.G.; Schulthess, T.C.; MacLaren, J.M. Spin-dependent tunneling conductance of Fe/MgO/Fe sandwiches. *Phys. Rev. B* **2001**, *63*, 054416:1–054416:12.
11. Djayaprawira, D.D.; Tsunekawa, K.; Nagai, M.; Maehara, H.; Yamagata, S.; Watanabe, N.; Yuasa, S.; Suzuki, Y.; Ando, K. 230% room-temperature magnetoresistance in CoFeB/MgO/CoFeB magnetic tunnel junctions. *Appl. Phys. Lett.* **2005**, *86*, 092502:1–092502:3.
12. Lee, Y.M.; Hayakawa, J.; Ikeda, S.; Matsukura, F.; Ohno, H. Giant tunnel magnetoresistance and high annealing stability in CoFeB/MgO/CoFeB magnetic tunnel junctions with synthetic pinned layer. *Appl. Phys. Lett.* **2006**, *89*, 042506:1–042506:3.
13. Lee, Y.M.; Hayakawa, J.; Ikeda, S.; Matsukura, F.; Ohno, H. Effect of electrode composition on the tunnel magnetoresistance of pseudo-spin-valve magnetic tunnel junction with a MgO tunnel barrier. *Appl. Phys. Lett.* **2007**, *90*, 212507:1–212507:3.
14. Isogami, S.; Tsunoda, M.; Komagaki, K.; Sunaga, K.; Uehara, Y.; Sato, M.; Miyajima, T.; Takahashi, M. *In situ* heat treatment of ultrathin MgO layer for giant magnetoresistance ratio with low resistance area product in CoFeB/MgO/CoFeB magnetic tunnel junctions. *Appl. Phys. Lett.* **2008**, *93*, 192109:1–192109:3.
15. Lee, D.H.; Lim, S.H. Increase of temperature due to Joule heating during current-induced magnetization switching of an MgO-based magnetic tunnel junction. *Appl. Phys. Lett.* **2008**, *92*, 233502:1–233502:3.
16. You, C.Y.; Ohkubo, T.; Takahashi, Y.K.; Hono, K. Boron segregation in crystallized MgO/amorphous-$Co_{40}Fe_{40}B_{20}$ thin films. *J. Appl. Phys.* **2008**, *104*, 033517:1–033517:6.
17. Chen, Y.T.; Wu, J.W. Effect of tunneling barrier as spacer on exchange coupling of CoFeB/AlO*x*/Co trilayer structures. *J. Alloys Compd.* **2011**, *509*, 9246–9248.
18. Jiang, L.; Nowak, E.R.; Scott, P.E.; Johnson, J.; Slaughter, J.M.; Sun, J.J.; Dave, R.W. Low-frequency magnetic and resistance noise in magnetic tunnel junctions. *Phys. Rev. B* **2004**, *69*, 054407:1–054407:9.
19. Ingvarsson, S.; Xiao, G.; Parkin, S.S.P.; Gallagher, W.J.; Grinstein, G.; Koch, R.H. Low-frequency magnetic noise in micron-scale magnetic tunnel junctions. *Phys. Rev. Lett.* **2000**, *85*, 3289–3292.
20. Nowak, E.R.; Merithew, R.D.; Weissman, M.B.; Bloom, I.; Parkin, S.S.P. Noise properties of ferromagnetic tunnel junctions. *J. Appl. Phys.* **1998**, *84*, 6195–6201.
21. Nowak, E.R.; Weissman, M.B.; Parkin, S.S.P. Electrical noise in hysteretic ferromagnet-insulator-ferromagnet tunnel junctions. *Appl. Phys. Lett.* **1999**, *74*, 600–602.
22. Nowak, E.R.; Spradling, P.; Weissman, M.B.; Parkin, S.S.P. Electron tunneling and noise studies in ferromagnetic junctions. *Thin Solid Films* **2000**, *377*, 699–704.
23. Ingvarsson, S.; Xiao, G.; Wanner, R.A.; Trouilloud, P.; Lu, Y.; Gallagher, W.J.; Marley, A.C.; Roche, K.P.; Parkin, S.S.P. Electronic noise in magnetic tunnel junctions. *J. Appl. Phys.* **1999**, *85*, 5270–5272.

24. Jonsson, T.; Nordblad, P.; Svedlindh, P. Dynamic study of dipole-dipole interaction effects in a magnetic nanoparticle system. *Phys. Rev. B* **1998**, *57*, 497–504.
25. Demir, S.; Zadrozny, J.M.; Nippe, M.; Long, J.R. Exchange coupling and magnetic blocking in bipyrimidyl radical-bridged dilanthanide complexes. *J. Am. Chem. Soc.* **2012**, *134*, 18546–18549.
26. Chen, Y.T.; Xie, S.M.; Jheng, H.Y. The low-frequency alternative-current magnetic susceptibility and electrical properties of Si(100)/$Fe_{40}Pd_{40}B_{20}$(*X* Å)/ZnO(500 Å) and Si(100)/ZnO(500 Å)/ $Fe_{40}Pd_{40}B_{20}$(*Y* Å) systems. *J. Appl. Phys.* **2013**, *113*, 17B303:1–17B303:3.
27. Yang, S.Y.; Chien, J.J.; Wang, W.C.; Yu, C.Y.; Hing, N.S.; Hong, H.E.; Hong, C.Y.; Yang, H.C.; Chang, C.F.; Lin, H.Y. Magnetic nanoparticles for high-sensitivity detection on nucleic acids via superconducting-quantum-interference-device-based immunomagnetic reduction assay. *J. Magn. Magn. Mater.* **2011**, *323*, 681–685.
28. Chen, Y.T.; Lin, S.H.; Lin, Y.C. Effect of low-frequency alternative-currentmagnetic susceptibility in $Ni_{80}Fe_{20}$ thin films. *J. Nanomater.* **2012**, *2012*, 186138:1–186138:6.
29. Chen, Y.T.; Chang, Z.G. Low-frequency alternative-current magnetic susceptibility of amorphous and nanocrystalline $Co_{60}Fe_{20}B_{20}$ films. *J. Magn. Magn. Mater.* **2012**, *324*, 2224–2226.
30. Feng, G.; Feng, J.F.; Coey, J.M.D. The effect of magnetic annealing on barrier asymmetry in $Co_{40}Fe_{40}B_{20}$/MgO magnetic tunnel junctions. *J. Magn. Magn. Mater.* **2010**, *322*, 1456–1459.